A Landsat Surface Reflectance Dataset for North America, 1990–2000

Jeffrey G. Masek, Eric F. Vermote, Nazmi E. Saleous, Robert Wolfe, Forrest G. Hall, Karl F. Huemmrich, Feng Gao, Jonathan Kutler, and Teng-Kui Lim

***Abstract*—The Landsat Ecosystem Disturbance Adaptive Processing System (LEDAPS) at the National Aeronautics and Space Administration (NASA) Goddard Space Flight Center has processed and released 2100 Landsat Thematic Mapper and Enhanced Thematic Mapper Plus surface reflectance scenes, providing 30-m resolution wall-to-wall reflectance coverage for North America for epochs centered on 1990 and 2000. This dataset can support decadal assessments of environmental and land-cover change, production of reflectance-based biophysical products, and applications that merge reflectance data from multiple sensors [e.g., the Advanced Spaceborne Thermal Emission and Reflection Radiometer, Multiangle Imaging Spectroradiometer, Moderate Resolution Imaging Spectroradiometer (MODIS)]. The raw imagery was obtained from the orthorectified Landsat GeoCover dataset, purchased by NASA from the Earth Satellite Corporation. Through the LEDAPS project, these data were calibrated, converted to top-of-atmosphere reflectance, and then atmospherically corrected using the MODIS/6S methodology. Initial comparisons with ground-based optical thickness measurements and simultaneously acquired MODIS imagery indicate comparable uncertainty in Landsat surface reflectance compared to the standard MODIS reflectance product (the greater of 0.5% absolute reflectance or 5% of the recorded reflectance value). The rapid automated nature of the processing stream also paves the way for routine high-level products from future Landsat sensors.**

***Index Terms*—Atmospheric correction, Landsat, remote sensing.**

I. Introduction

THE analysis of land-cover change and disturbance across large areas remains a central goal for Earth Science research. Changes in vegetation patterns affect Earth's climate, by altering albedo, evapotranspiration, and carbon exchange with the atmosphere [1]–[3]. At the same time, many land-cover changes (such as deforestation and agricultural expansion) directly reflect alteration of ecosystems by human populations, with clear impacts on biodiversity and ecosystem health. It is well known that monitoring land-cover change requires high-resolution imagery ($\sim$ 30-m resolution or better) in order to accurately quantify areas and rates of change [4]. For these reasons, the Global Climate Observing System (GCOS) has called for routine analysis of global land-cover patterns at 30-m resolution every five years.

Manuscript received May 26, 2005; revised July 5, 2005.

J. G. Masek, N. E. Saleous, R. Wolfe, F. Gao, J. Kutler, and T.-K. Lim are with the Biospheric Sciences Branch, NASA Goddard Space Flight Center, Greenbelt, MD 20771 USA (e-mail: jeffrey.g.masek@nasa.gov).

E. F. Vermote is with the University of Maryland, College Park, MD 20742 USA and also with the NASA Goddard Space Flight Center, Greenbelt, MD 20771 USA.

F. G. Hall and K. F. Huemmrich are with the University of Maryland Baltimore County, Baltimore, MD 21250 USA.

Digital Object Identifier 10.1109/LGRS.2005.857030

Such an ambitious goal requires rapid, automated approaches to preprocessing and analyzing high-resolution remote sensing datasets. The National Aeronautics and Space Administration (NASA) has taken the first step toward this goal by procuring the Landsat GeoCover product from Earth Satellite Corporation as part of the Science Data Purchase program. The GeoCover dataset is a global collection of orthorectified, mostly cloud-free Landsat imagery, centered on 1975, 1990, and 2000 epochs [5]. Actual image acquisition dates may vary depending on data availability, but for North America most acquisitions date from 1987–1992 for the 1990-epoch coverage, and 1999–2001 for the 2000-epoch coverage. Since the data have been georegistered and orthorectified (to a geodetic accuracy of $\sim$ 60 m), this product partly supports decadal change-detection applications. However, no radiometric processing was attempted for the GeoCover product beyond normal Landsat Level 1G processing.

The Landsat Ecosystem Disturbance Adaptive Processing System (LEDAPS) project was funded in 2004 to assemble a record of ecosystem disturbance for North America, using the Landsat GeoCover product, in support of the upcoming North American Carbon Program (NACP) [6]. As part of that effort, the LEDAPS team has calibrated and atmospherically corrected the 1990 and 2000 GeoCover product for North America. These data, comprising some 2100 Landsat Thematic Mapper (TM) and Enhanced TM Plus (ETM+) scenes, are available for download from the LEDAPS web site.[1] The new surface reflectance dataset should help researchers more easily use the GeoCover data for tracking land-cover changes in North America, including fire, forest harvest, urbanization, woody encroachment, and changes in agriculture. The purpose of this letter is to document the processing approach used to create the North American surface reflectance product, present initial studies of its accuracy and precision, and illustrate relevant applications of the product.

II. LEDAPS Reflectance Processing Objectives

The processing goals for the LEDAPS surface reflectance product flowed from the overall goal of mapping disturbance across North America. It was decided that radiometric change-detection methods (as opposed to comparisons of classified imagery) would yield best results. To facilitate change detection, it was also decided to correct each image to directional surface reflectance, a physically based measure of land-surface properties that can be compared with similar observations from MODIS and other Earth Observation System (EOS) instruments. Since

[1]http://ledaps.nascom.nasa.gov/ledaps/ledaps_NorthAmerica.html

the Landsat instruments always acquire imagery within $\pm 7.5^\circ$ of nadir, variation in the bidirectional reflectance distribution function (BRDF) from changing view angles was not a concern. However, the GeoCover images were acquired at various points in the growing season, and changes in both phenology and BRDF (from Sun angle variations) do result.

III. Processing Description

The LEDAPS project reused the MODAPS software architecture developed at the NASA Goddard Space Flight Center (GSFC) for producing higher level products from MODIS Level 1B data [7]. In this architecture, low-level data (digital numbers, or DN) are ingested (using HDF-EOS file formats), calibrated to at-sensor radiance, atmospherically corrected to surface reflectance using the 6S approach [8], [9], and then composited, gridded, and/or reprojected as required. Higher level products (such as forest disturbance maps) may then be created from the surface reflectance datasets.

A. Ingest and Calibration

Landsat GeoCover data products were ingested from the University of Maryland Global Land Cover Facility via FTP. Level 1G ETM+ data were calibrated to at-sensor radiance (watts per square meter per steradian per micron) using the published coefficients from the Landsat-7 online Science User's Handbook (http://ltpwww.gsfc.nasa.gov/IAS/handbook/handbook_toc.html; see also [10]). The calibration procedure for Landsat-5 TM GeoCover images was more involved. Landsat-5 TM products produced from the NLAPS processing system at the Canada Centre for Remote Sensing or the U.S. Geological Survey EROS Data Center before May 2003 were calibrated using scene-specific onboard calibrator lamp brightness values. These values, which vary considerably from day to day, probably reflect a long-term degradation in sensor performance superposed on short-term, random variations in lamp output. Immediately after the launch of Landsat-7 in 1999, an underfly experiment allowed both Landsat-7 ETM+ and Landsat-5 TM to simultaneously image the same terrain. With this added control, the Landsat-5 TM historic calibration was revised in 2003 to use a simple exponential decay model [11], [12]. Since the 1990-epoch GeoCover products were processed to Level 1G during 1998–2000, they were originally calibrated using the "old," lamp-based calibration. For LEDAPS, we used the averaged daily lamp brightness history to remove the original, erroneous calibration, and then applied the revised calibration coefficients for the appropriate image acquisition date.

Calibrated images were then corrected to top-of-atmosphere (TOA) reflectance by correcting for solar zenith, Sun–Earth distance, TM or ETM+ bandpass, and solar irradiance (using the MODTRAN solar output model). Landsat TOA reflectance products were output in HDF-EOS format, and may be downloaded from the LEDAPS web site.

B. Atmospheric Correction

Atmospheric correction seeks to compensate for scattering and absorption of radiance by atmospheric constituents, yielding an accurate estimate of surface reflectance. The Landsat surface reflectance product is derived from TOA reflectance by applying an atmospheric correction scheme that assumes that: 1) the target is Lambertian and infinite and 2) the gaseous absorption and particle scattering in the atmosphere can be decoupled. The TOA reflectance can be expressed as

$$\rho_{\mathrm{TOA}} = T_g(\mathrm{O_3}, \mathrm{O_2}, \mathrm{CO_2}, \mathrm{NO_2}, \mathrm{CH_4}) \times \left[\rho_{R+A} + T_{R+A} T_g(\mathrm{H_2O}) \frac{\rho_s}{1 - S_{R+A}\rho_s} \right] \quad (1)$$

where ρ_s is the surface reflectance, T_g is the gaseous transmission due to the gases listed between parentheses, T_{R+A} is Rayleigh and aerosol transmission, ρ_{R+A} is the Rayleigh and aerosols atmospheric intrinsic reflectance, and S_{R+A} is the Rayleigh and aerosols spherical albedo. The transmission, intrinsic reflectance, and spherical albedo terms are computed using the 6S radiative transfer code [8]. Ozone concentrations are derived from Total Ozone Mapping Spectrometer (TOMS) data aboard the Nimbus-7, Meteor-3, and Earth Probe platforms. The gridded TOMS ozone products are available at a resolution of 1.25° longitude and 1.00° latitude from the NASA GSFC Data Active Archive Center (DAAC). In cases where TOMS data are not available (e.g., 1994–1996), NOAA's Tiros Operational Vertical Sounder (TOVS) ozone data are used. Column water vapor is taken from NOAA National Centers for Environmental Prediction (NCEP) reanalysis data available at a resolution of $2.5^\circ \times 2.5^\circ$ (http://dss.ucar.edu/datasets/ds090.0/). Digital topography (1 km GTopo30) and NCEP surface pressure data are used to adjust Rayleigh scattering to local conditions.

Like other atmospheric correction schemes for MODIS and Landast, we make use of the dark, dense vegetation (DDV) method of Kaufman *et al.* [13] in order to extract aerosol optical thickness (AOT) directly from the imagery [8], [9], [14], [15]. Based on the physical correlation between chlorophyll absorption and bound water absorption, this method postulates a linear relation between shortwave-infrared (2.2 mm) surface reflectance (nearly unaffected by the atmosphere) and surface reflectance in the visible bands. By using the relation to calculate surface reflectance for the visible bands, and comparing the result to the TOA reflectance, aerosol optical depth may be estimated.

For LEDAPS AOT estimation, each image is subaveraged to 1-km resolution (to suppress local heterogeneity), and candidate "dark targets" with TOA $\rho_7 < 0.15$ are selected. For these targets, we assume a correlation only between the blue (0.45–0.52) and SWIR (2.2) bands, such that $\rho_{\mathrm{BLUE}} = 0.33(\rho_{\mathrm{SWIR}})$. Water targets are excluded. The specific relation is derived from an analysis of data from Aerosol Robotic Network (AERONET) sites where AOT is measured directly (Fig. 1). The calculated AOT in the blue wavelengths is propagated across the spectrum using a continental aerosol model. Aerosol optical thickness for each band is interpolated spatially between the dark targets using a spline algorithm. The interpolated AOT, ozone, atmospheric pressure, and water vapor are supplied to the 6S radiative transfer algorithm, which then inverts TOA reflectance for surface reflectance for each 30-m pixel.

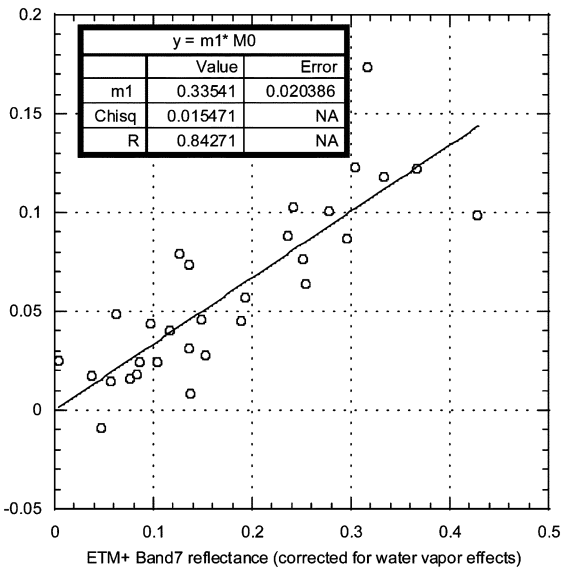

Fig. 1. Observed linear relation between ETM+ band 7 (2.09–2.35 μm) and band 1 (0.45–52 μm) for local regions near 21 AERONET sites, supporting the Kaufmann *et al.* [13] approach for aerosol extraction. Atmospheric correction for these targets was performed using 6S radiative transfer model, and aerosol optical thickness derived from simultaneous AERONET observations.

Fig. 2. Example of LEDAPS atmospheric correction. (a) Top-of-atmosphere (TOA) reflectance composite (bands 3,2,1) for Landsat-7 ETM+ image of San Francisco Bay (July 7, 1999); (b) Surface reflectance composite. Both images are linearly scaled from $\rho = 0.0$ to 0.15.

The TOA and surface reflectance maps preserve the 30-m resolution of the original GeoCover data, which were originally projected to UTM using the WGS-84 datum (Fig. 2). An additional 500-m resolution product has also been prepared by aggregating (averaging) the 30-m reflectance data to Lambert azimuthal equal area projection. This coarse-resolution grid may be useful for direct comparison with MODIS reflectance products.

To date, no adjustments for BRDF (due to solar and topographic geometry), or phenology have been attempted for the LEDAPS surface reflectance dataset. While these adjustments can facilitate comparison of imagery from different seasons, most published algorithms remain empirical in nature [16], [17]. Specifically, these algorithms require some prior knowledge of land-cover type so the appropriate BRDF response and/or phenology trend can be applied.

C. Data Processing, Formats, and Distribution

LEDAPS runs on a distributed cluster of Intel processors running the Linux operating system. Job handling is performed on a per-scene basis (i.e., one processor per scene). The system can process a single Landsat scene to surface reflectance at the rate of one scene per processor per hour, such that the entire North American GeoCover product suite (TM and ETM+) can be reprocessed in $\sim$9 days using the current hardware configuration.

Files at 30- and 500-m resolutions are available from the LEDAPS web site via FTP. Calculated surface reflectance values are stored as 16-bit integers (reflectance factor multiplied by 10 000) in HDF-EOS format. The HDF-EOS data structures contain one layer for each reflective band (excluding the thermal infrared), an aerosol optical thickness map for the blue band, and a "QA" layer with separate flags for clouds, missing data, and data originating from Landsat-4. Each full-resolution surface reflectance file is ~ 1.3 GB uncompressed, or about 500 MB compressed.

IV. Surface Reflectance Characteristics and Validation

The following three approaches are being utilized to assess the quality of LEDAPS products:

1) comparison between LEDAPS ETM+ surface reflectance and simultaneously acquired Terra MODIS daily reflectance products (MOD09GHK);
2) comparison between Landsat image-derived aerosol optical thickness values and simultaneous AERONET AOT retrievals;
3) comparison between Landsat surface reflectance values and vicarious retrievals from high-resolution imagery or airborne radiometer data.

Each validation approach has unique strengths and weaknesses. Comparisons with MODIS can be applied to a large volume of ETM+ imagery, but are somewhat circular since the LEDAPS and MODIS atmospheric correction algorithms use the same 6S radiative transfer model. The second method is useful as an independent check on the DDV AOT retrievals, but does not offer validation of the full atmospheric correction. The final approach can only be applied to a handful of locations where vicarious retrievals have occurred, and data quality of these retrievals may be problematic. To date, only the first two validation approaches have been completed.

A. MODIS Comparisons

The Terra MODIS09 daily reflectance product is acquired within 15 min of the corresponding Landsat-7 ETM+ image, with the same viewing geometry since Terra and Landsat-7 share the same orbit. MODIS also includes spectral bands equivalent to those on ETM+ although the exact bandpasses differ. For LEDAPS validation, MODIS 500-m surface reflectance products were processed from individual swaths,

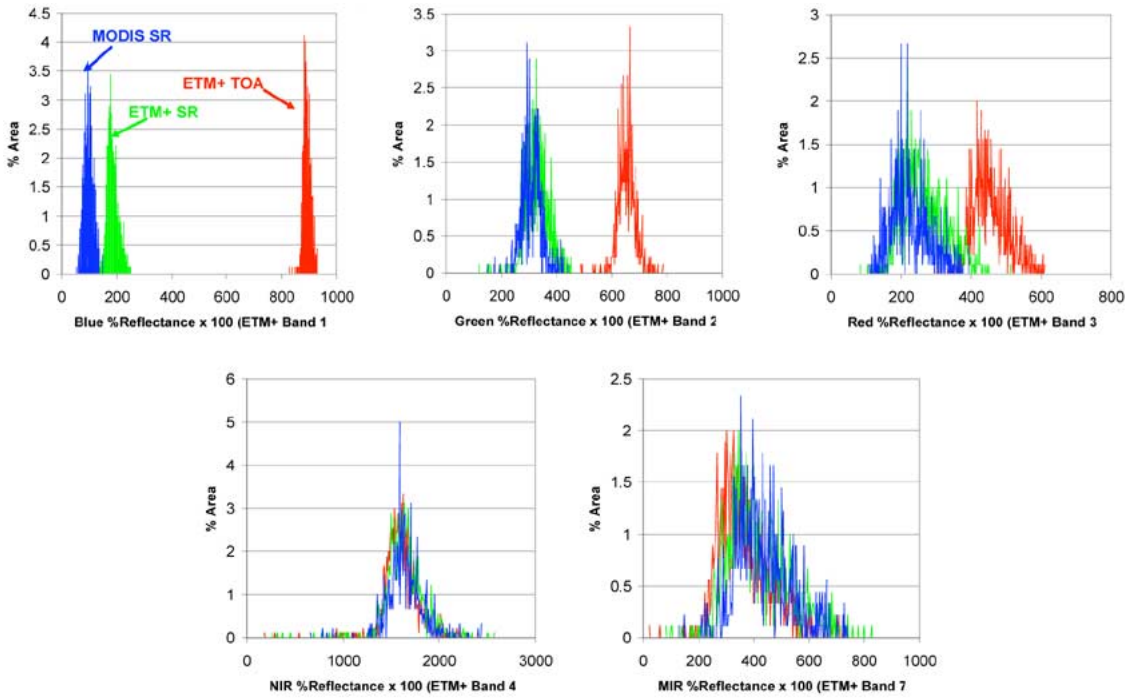

Fig. 3. Histograms of TOA reflectance from Landsat, surface reflectance from MODIS, and surface reflectance from Landsat, from a 15 × 15 km region in Saskatchewan, for Landsat bands 1, 2, 3, 4, and 7. Both MODIS and Landsat images were acquired on September 17, 2001.

and registered with Landsat-7 ETM+ reflectance images acquired within 15 min. The Landsat reflectance products were aggregated to 500-m resolution by averaging blocks of pixels. For one scene in Saskatchewan, Canada, three visually homogenous subwindows from each dataset were extracted and compared.

Plotting histograms before and after correction for each subwindow suggests that, for most spectral bands, differences between MODIS and ETM+ surface reflectance values are small for vegetated targets (Fig. 3). One exception is the blue band, where ETM+ values trend $\sim 1\%$ higher than the comparable MODIS band. In the green and red bands, ETM+ values trend $\sim$0.5% higher than comparable MODIS bands. Consistent trends in the near-infrared and shortwave-infrared are difficult to detect due to the spread of the data. These differences appear to be within the uncertainty of the MODIS surface reflectance product (the greater of 0.5% absolute reflectance or 5% of the recorded reflectance value) for normal aerosol loadings $(\tau_{550\,\mathrm{nm}} < 0.5)$. The effects of differing spectral bandpasses between Landsat ETM+ and MODIS were examined by creating vegetation spectra for a range of leaf-area index (LAI) values using Kubelka–Munk theory and leaf optical data for spruce, and sampling those spectra with the appropriate spectral response curve. The derived reflectance values were compared with those from Fig. 3, which also sampled predominately spruce forest. The results suggest that discrepancies between ETM+ and MODIS values are not readily explained by bandpass differences alone (Table I), but instead record inherent uncertainties in the atmospheric correction procedure.

TABLE I
PREDICTED AND OBSERVED VALUES OF $\Delta\rho(=\rho_{\mathrm{MODIS}}-\rho_{\mathrm{ETM}})$. PREDICTED VALUES OF $\Delta\rho$ DERIVED FROM MODIS AND LANDSAT-7 ETM+ RELATIVE SPECTRAL RESPONSE CURVES SAMPLING A TYPICAL SPRUCE VEGETATION SPECTRUM

Landsat band	wavelength (μm)	ρ_{MODIS} observed	$\rho_{\mathrm{ETM+}}$ observed	Δρ observed	Δρ predicted
1	0.45-0.52	0.97	1.84	-0.9	-0.2
2	0.53-0.61	3.09	3.30	-0.2	0.4
3	0.63-0.69	2.27	2.64	-0.4	0.2
4	0.78-0.90	16.61	16.51	0.1	0.1

B. AERONET AOT Comparisons

AERONET is a global network of Sun photometers used to observe aerosol amount and properties, and to calibrate remote sensing measurements of aerosols [18]. Several of these records extend back to the early 1990s. Observations from 21 of these sites in North America were compared with simultaneous AOT estimates obtained using the image-based approach discussed above (Fig. 4).

The results show reasonable agreement between the LEDAPS image-based AOT estimates and AERONET observations. For comparison, empirical uncertainty in MODIS land AOT retrievals $(\Delta\mathrm{AOT})$ is proportional to the retrieved value, such that

$$\Delta\mathrm{AOT}_{\mathrm{MODIS}} = 0.05 + 0.2^{*}\mathrm{AOT}_{\mathrm{MODIS}}. \tag{2}$$

Plotting this relation on Fig. 4 indicates comparable performance of the DDV retrieval algorithm whether using MODIS data or Landsat data. This uncertainty is also consistent with that of the DDV SWIR-visible reflectance correlation (Fig. 1) [13]. Visual inspection of the LEDAPS AOT distributions, however, suggests that land-cover type may influence the aerosol retrievals, with somewhat higher AOT values occurring over urban and other bright targets. This may be caused by excess path radiance scattered into the line of sight by nearby bright targets (the adjacency effect). Future work will investigate the feasibility of correcting the AOT maps for adjacency effects.

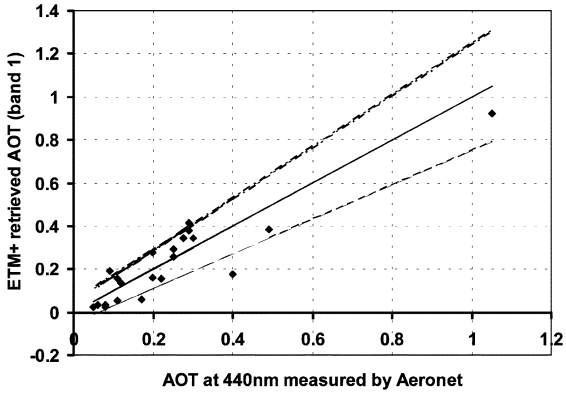

Fig. 4. Retrieved ETM+ aerosol optical thickness values from LEDAPS dataset regressed against simultaneous AERONET AOT values for the blue (0.45–0.52 μm) band. (Solid line) One-to-one line. (Dashed lines) MODIS AOT uncertainties of $(0.05 + 0.2^{*}\text{AOT})$.

C. Known Issues and Future Work

The validation studies have illuminated several deficiencies in the reflectance product, which will be corrected in future releases. Clouds are currently masked using the Landsat-7 Automatic Cloud-cover Assessment (ACCA) algorithm [19]. While ACCA has performed well for providing scene-level cloud-cover metadata for the Landsat-7 program, it has not proven reliable for creating cloud masks as part of LEDAPS. Also, some overestimation of aerosols due to adjacency effects or deviations from the DDV relation has led to occasional negative reflectance values.

Future product releases will also extend the LEDAPS surface reflectance suite back the 1975-era MSS GeoCover dataset. Since older MSS data cannot be reliably calibrated or atmospherically corrected, each scene from the 1975-era MSS archive will be radiometrically rectified to the ETM+ image as in [20].

V. Discussion: Dataset Applications and Future Directions

The LEDAPS surface reflectance dataset for North America supports multiple uses, including mapping of land-cover, decadal land-cover change, surface water resources, and vegetation biophysics. The conversion to reflectance specifically allows users to cross-compare Landsat observations to laboratory or ground-measured spectral curves, reflectance data from other instruments (ASTER, MODIS, MISR), or the output from canopy reflectance models. None of these techniques was feasible with the original GeoCover dataset. In particular, the cross-comparison between MODIS and Landsat supports scaling studies that seek to understand how radiometric and biophysical properties derived at MODIS resolution (500–1000 m) scale to Landsat resolution (30 m).

In the long term, the LEDAPS exercise points the way toward fully operational atmospheric correction of Landsat-type imagery. Such an approach has already been pioneered by the ASTER science team as part of the EOS program, for a limited set of "on-demand" requests. Since 1972, the Landsat program has never had a standard physical product associated with the mission—only calibrated digital numbers. It is reasonable to expect that data centers, running LEDAPS-like processing systems, could produce a range of standard land science products based on surface reflectance imagery from future Landsat sensors. Such an effort would make routine the seemingly ambitious goal of updating the world's knowledge of land-cover characteristics every five years.

References

[1] A. C. Janetos and C. O. Justice, "Land cover and global productivity: A measurement strategy for the NASA programme," *Int. J. Remote Sens.*, vol. 21, pp. 1491–1512, 2000.

[2] R. A. Houghton, "The annual net flux of carbon to the atmosphere from changes in land use 1850–1990," *Tellus Series B-Chem. Phys. Meteorol.*, vol. 51, pp. 298–313, 1999.

[3] R. S. DeFries, L. Bounoua, and G. J. Collatz, "Human modification of the landscape and surface climate in the next fifty years," *Global Change Biol.*, vol. 8, pp. 438–458, 2002.

[4] J. R. G. Townshend and C. O. Justice, "Selecting the spatial-resolution of satellite sensors required for global monitoring of land transformations," *Int. J. Remote Sens.*, vol. 9, pp. 187–236, 1988.

[5] C. J. Tucker, D. M. Grant, and J. D. Dykstra, "NASA's global orthorectified Landsat data set," *Photogramm. Eng. Remote Sens.*, vol. 70, pp. 313–322, 2004.

[6] S. C. Wofsy and R. C. Harriss, "The North American Carbon Program (NACP) Report of the NACP Committee of the U.S. Interagency Carbon Cycle Science Program," U.S. Global Change Res. Program, Washington, DC, 2002.

[7] C. O. Justice, J. R. G. Townshend, E. F. Vermote, E. Masuoka, R. E. Wolfe, N. Saleous, D. P. Roy, and J. T. Morisette, "An overview of MODIS land data processing and product status," *Remote Sens. Environ.*, vol. 83, no. 1–2, pp. 3–15, 2002.

[8] E. F. Vermote *et al.*, "Atmospheric correction of visible to middle-infrared EOS-MODIS data over land surfaces: Background, operational algorithm, and validation," *J. Geophys. Res.*, vol. 102, pp. 17131–17 141, 1997.

[9] E. F. Vermote, N. Saleous, and C. O. Justice, "Atmospheric correction of MODIS data in the visible to middle infrared: First results," *Remote Sens. Environ.*, vol. 83, pp. 97–111, 2002.

[10] B. L. Markham, K. J. Thome, J. A. Barsi, E. Kaita, D. L. Helder, J. L. Barker, and P. L. Scaramuzza, "Landsat-7 ETM+ on-orbit reflective-band radiometric stability and absolute calibration," *IEEE Trans. Geosci. Remote Sens.*, vol. 42, no. 12, pp. 2810–2820, Dec. 2004.

[11] P. M. Teillet, D. L. Helder, T. A. Ruggles, R. Landry, F. J. Ahern, N. J. Higgs, J. Barsi, G. Chander, B. L. Markham, J. L. Barker, K. J. Thome, J. R. Schott, and F. D. Palluconi, "A definitive calibration record for the Landsat-5 Thematic Mapper anchored to the Landsat-7 radiometric scale," *Can. J. Remote Sens.*, vol. 30, pp. 631–643, 2004.

[12] G. Chander, D. L. Helder, B. L. Markham, J. D. Dewald, E. Kaita, K. J. Thome, E. Micijevic, and T. A. Ruggles, "Landsat-5 TM reflective-band absolute radiornetric calibration," *IEEE Trans. Geosci. Remote Sens.*, vol. 42, no. 12, pp. 2747–2760, Dec. 2004.

[13] Y. J. Kaufman, A. E. Wald, L. A. Remer, B.-C. Gao, R.-R. Li, and L. Flynn, "The MODIS 2.1 μm channel—Correlation with visible reflectance for use in remote sensing of aerosol," *IEEE Trans. Geosci. Remote Sens.*, vol. 35, no. 5, pp. 1286–1298, Sep. 1997.

[14] H. Ouaidrari and E. F. Vermote, "Operational atmospheric correction of Landsat TM data," *Remote Sens. Environ.*, vol. 70, pp. 4–15, 1999.

[15] S. Liang *et al.*, "An operational atmospheric correction algorithm for Landsat Thematic Mapper imagery over the land," *J. Geophys. Res.*, vol. 102, pp. 17 173–17 186, 1997.

[16] J. D. Shepherd and J. R. Dymond, "BRDF correction of vegetation in AVHRR imagery," *Remote Sens. Environ.*, vol. 74, pp. 397–408, 2000.

[17] J. Cihlar, J. Chen, Z. Li, R. Latifovic, G. Fedosejevs, M. Adair, W. Park, R. Fraser, A. Trishchenko, B. Guindon, D. Stanley, and D. Morse, "GeoComp-n, an advanced system for the processing of coarse and medium resolution satellite data Part 2: Biophysical products for Northern ecosystems," *Can. J. Remote Sens.*, vol. 28, pp. 21–44, 2002.

[18] B. N. Holben *et al.*, "AERONET—A federated instrument network and data archive for aerosol characterization," *Remote Sens. Environ.*, vol. 66, pp. 1–16, 1998.

[19] R. Irish, "Landsat7 automatic cloud cover assessment, in algorithms for multispectral, hyperspectral, and ultraspectral imagery," *Proc. SPIE*, vol. 4049, 2000.

[20] F. G. Hall, D. E. Strebel, J. E. Nickeson, and S. J. Goetz, "Radiometric rectification: Toward a common radiometric response among multidate, multisensor images," *Remote Sens. Environ.*, vol. 35, pp. 11–27, 1991.